Electronic Supplementary Material (ESI) for New Journal of Chemistry.

Supporting Information (SI)

Synthesis of highly dispersed Nb_2O_5-graphene heterojunction composite using ethylene diamine tetraacetic acid and boron-functionalized graphene quantum dot for flexible symmetrical supercapacitors with ultrahigh energy density

Liu Xiaoyue, Xu Pengwu, Li Ruiyi, Zhu Haiyan, Liu Xiaohao and Li Zaijun*

Key Laboratory of Synthetic and Biological Colloids, Ministry of Education, School of Chemical and Material Engineering, and School of Life Science and Health Engineering, Jiangnan University, Wuxi 214122, China

1. Experimental

1.1. Materials and reagents

Niobium pentachloride ($NbCl_5$), citric acid, ethylenediamine, ethylenediamine tetraacetic acid (EDTA), boric acid (H_3BO_3) and ascorbic acid (AA) were purchased from Sigma-Aldrich Chemical Company. Graphite oxide (GO) was prepared from natural graphite by the modified Hummers' method [1]. The solid electrolyte (PVA/Li_2SO_4) was prepared by adding 2.0 g of polyvinyl alcohol (PVA) in 20 mL of ultrapure water [1]. Kept it at room temperature for 24 h and then heated at 75°C with stirring until a clear homogeneous solution was formed. After that, dropped 10 mL of 3 mol L^{-1} Li_2SO_4 solution under stirring and cool down to room temperature. Silver nanowires (Ag NW) in isopropanol (5 mg mL^{-1}) was purchased from Jiangsu XFNANO Materials Tech Co., Ltd. A n-Nb_2O_5-p-GQD-G ink was prepared by dispersing a solid sample containing 80 wt.% n-Nb_2O_5-p-GQD-G and 20 wt.% acetylene black in the above solid electrolyte under ultrasonication.

1.2. Material characterization

Scanning electron microscope (SEM) was carried out in HITACHI S4800 field emission scanning electron microscope. Transmission electron microscope (TEM) was conducted on a JEOL 2010 transmission electron microscope at 200 keV. High-angle annular dark field scanning transmission electron microscopy (HAADF-STEM) was conducted by FEI Themis Z microscope with 200 kV accelerating voltage. STEM samples were prepared by depositing a droplet of suspension onto a Cu grid coated with lacey carbon film. The sample was prepared by dispensing a small amount of dry powder in ethanol. Then, one drop of the suspension was dropped on 300 mesh copper. The TEM grid covered with thin amorphous carbon film. X-ray diffraction (XRD) pattern was measured on the X-ray D8 Advance Instrument operated at 40 kV and 20 mA and using Cu Kα radiation source with λ=0.15406 nm. X-Ray photoelectron spectroscopy (XPS) were carried out in a PHI 5700 ESCA spectrometer with mono chromated Al KR radiation.

2.3. Electrochemical measurements

Three-electrode test system and flexible supercapacitor were employed for evaluating the supercapacitor performance of n-Nb_2O_5-p-GQD-G. In the three-electrode testing system, the titanium sheet (1cm×1cm) bearing n-Nb_2O_5-p-GQD-G, platinum foil (1cm×1cm) and saturated calomel electrode were used as working electrode, counter electrode and reference electrode, respectively. A 1.0 mol L^{-1} Li_2SO_4 aqueous solution was used as an electrolyte. The working electrode was constructed by coating the mixture of 85 wt.% n-Nb_2O_5-p-GQD-G, 10 wt.% acetylene black and 5wt.% polyvinylidene fluoride as a binder dissolved in N-methyl-pyrrolidone. The active mass coated on the each of titanium sheet electrodes was in the range of 1-2 mg cm^{-2}. Before use, the electrodes were dried in vacuum at 85 °C for 24 h.

Cyclic voltammogram (CV), electrochemical impedance spectroscopy (EIS) and galvanostatic charge/discharge curves of three-electrode testing system and flexible supercapacitor were measured on the CHI 660D electrochemical workstation. The potential amplitude of ±5 mV and frequency of 0.01-10^5 Hz were adopted in the EIS measurements. For the three-electrode system, the specific capacitance (C_g, based on a single electrode) were calculated according to the equation (1) [3]:

$$C_g = \frac{It}{m\Delta V} \quad (1)$$

Here, C_g is the gravimetric capacitance (F g^{-1}), I is the current (A), m is the active mass on the electrode (g), ΔV is the potential range, and t is the discharging time. For the symmetric supercapacitor, the specific capacitance (C_{g2}), energy density and power density were calculated according to the equations (2, 3 and 4) [4]:

$$C_{g2} = \frac{2It}{m\Delta V} \quad (2)$$

$$E_g = \frac{C_{g2}\Delta V^2}{8 \times 3600} \quad (3)$$

$$P_g = \frac{E_{g2} \times 3600}{t_{discharge}} \quad (4)$$

Here, C_g is the gravimetric capacitance (F g^{-1}) of a single electrode in two-electrode cell. Furthermore, E_g (W h g^{-1}) and P_g (W g^{-1}) are the gravimetric energy density and gravimetric power density, respectively, based on the total active material in the cell. I is the current (A), m is the active mass of active material in a single electrode (g), ΔV is the potential range, and t is the discharging time.

2. Figures

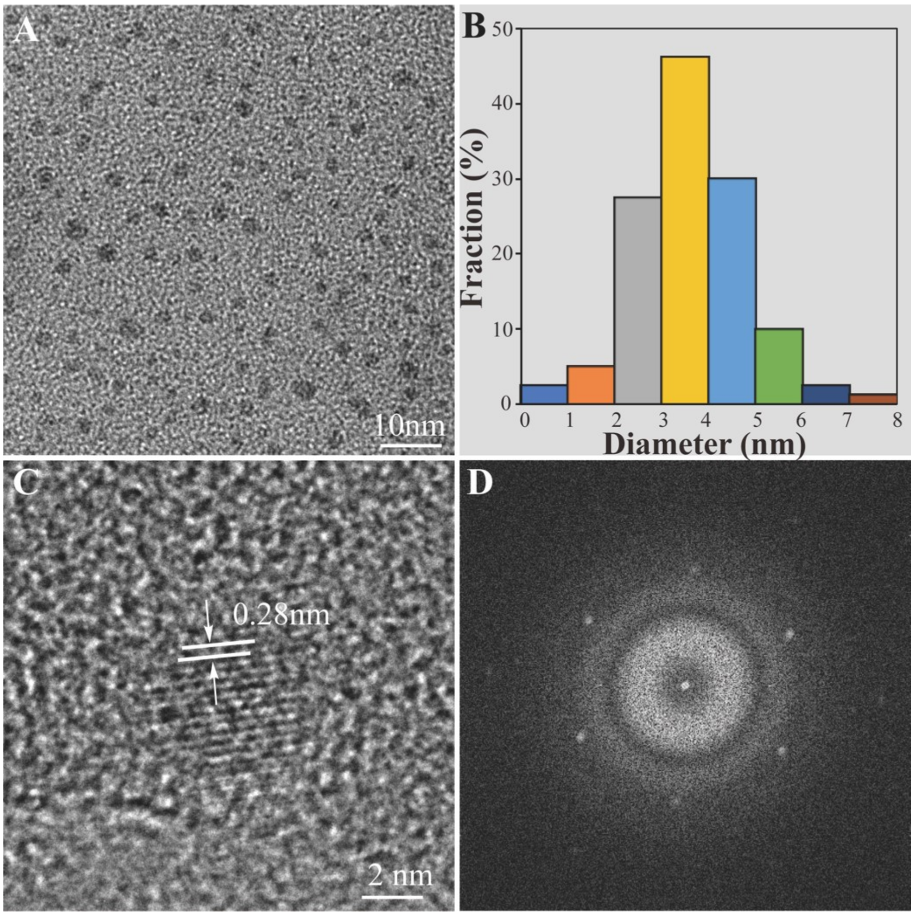

Fig. s1 TEM image(A), particle size distribution (B), HRTEM (C) and electron diffraction pattern (D) of the as-synthesized p-GQD

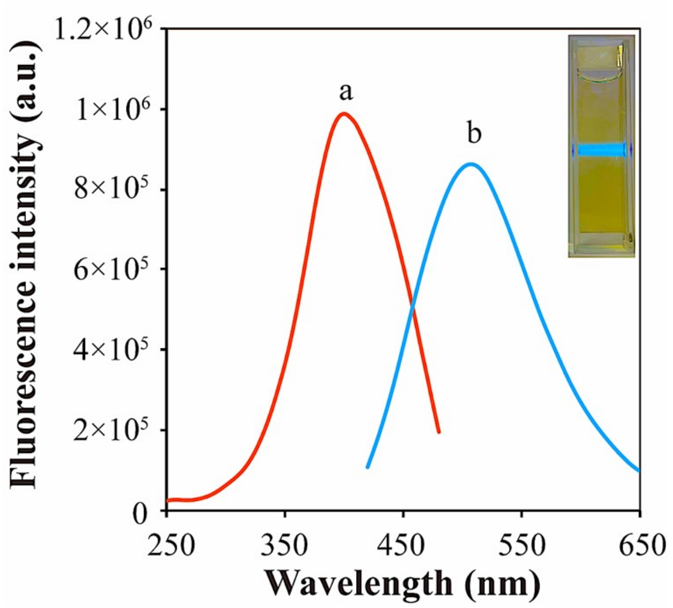

Fig. s2 The fluorescence excitation spectrum (a) and emission spectrum (b)of p-GQD

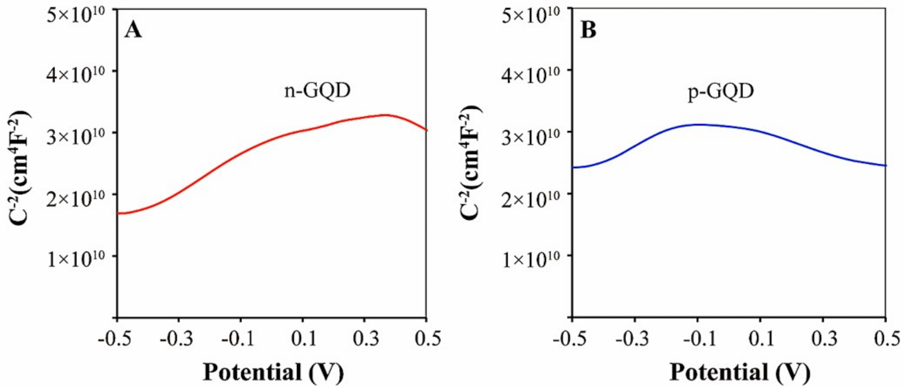

Fig. s3 The Mott-Schottky plots of n-GQD and p-GQD

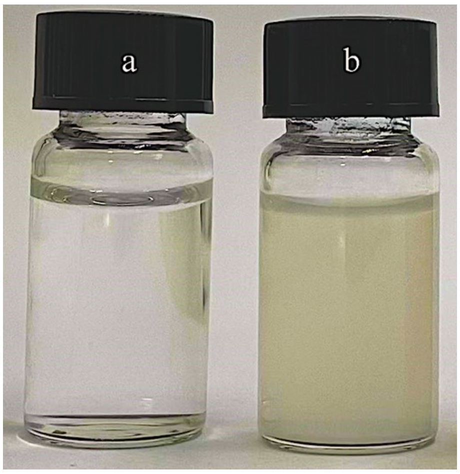

Fig. s4 Optical photographs of water (a) and $NbCl_5$ aqueous solution (b)

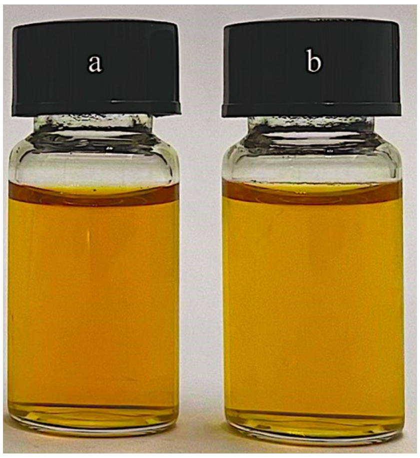

Fig. s5 Optical photographs of p-GQD aqueous solution (a) and $NbCl_5$ in p-GQD aqueous solution (b)

Fig. s6 Optical photographs of p-GQD before (a) and after added p-GQD/GO (b), $NbCl_5$ (c) and ascorbic acid (d)

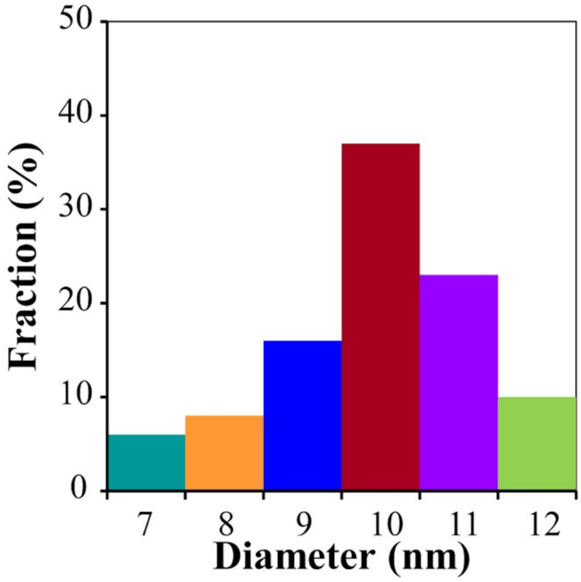

Fig. s7 The length distribution of Nb_2O_5 nanorods in n-Nb_2O_5-p-GQD-G

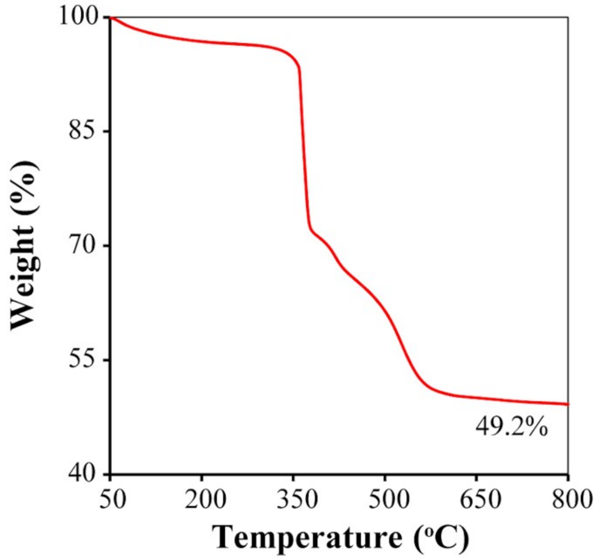

Fig. s8 Thermogravimetric curve of n-Nb_2O_5-p-GQD-G

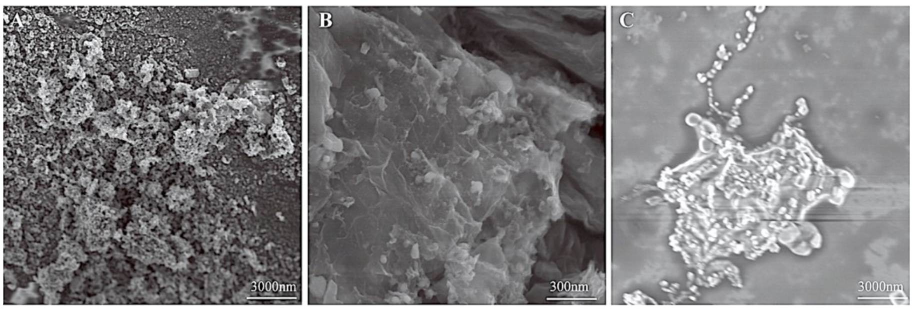

Fig. s9 The SEM images of Nb2O5 nanoparticles formed in the absence of p-GQD and GO (A), p-GQD (B) and GO (C)

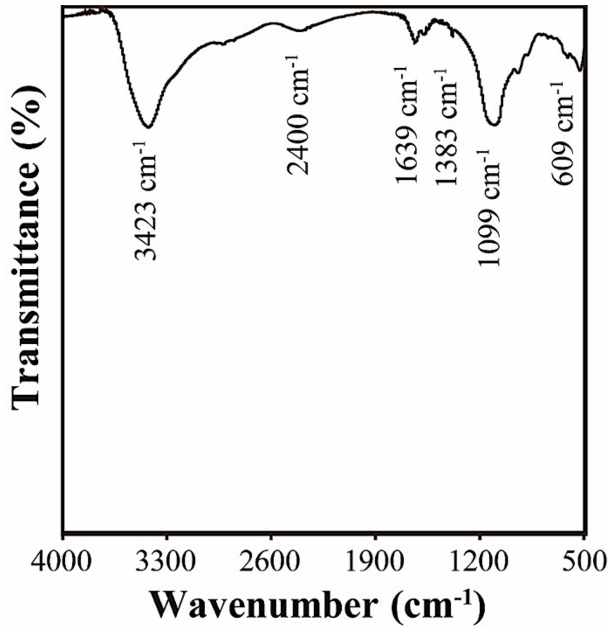

Fig. s10 IR spectrum of n-Nb_2O_5-p-GQD-G

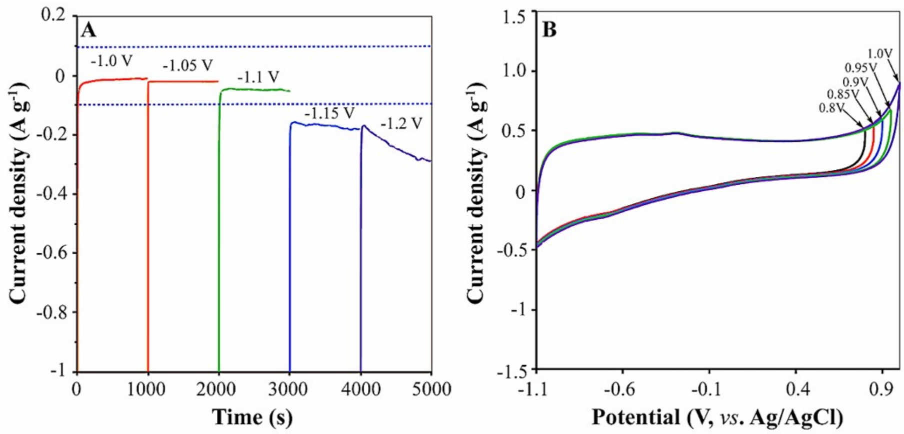

Fig. s11 Chronoamperometry curves (A) of n-Nb_2O_5-p-GQD-G electrode in 1 M Li_2SO_4 electrolyte at various potentials and CV curves (B) in 1 M Li_2SO_4 electrolyte of n-Nb_2O_5-p-GQD-G electrode within various potential ranges

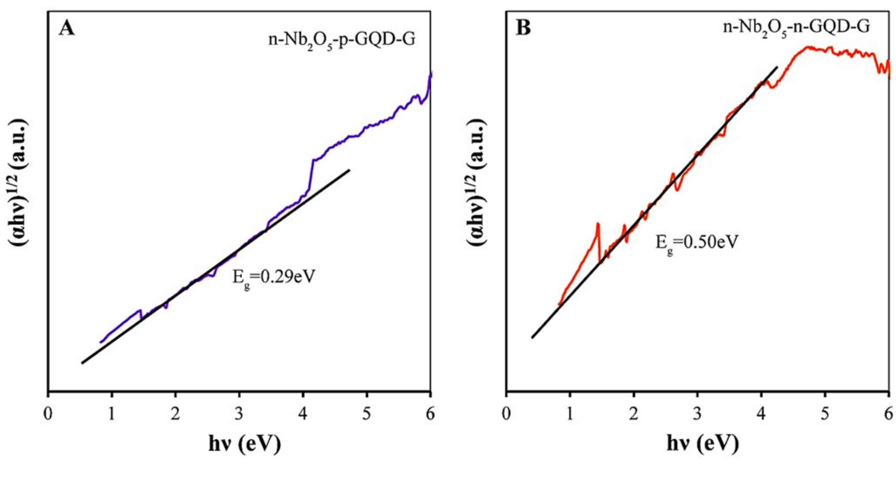

Fig. s12 The relationship curves of $(\alpha h\nu)^{1/2}$ with $h\nu$ for n-Nb_2O_5-p-GQD-G (A) and n-Nb_2O_5-n-GQD-G (B)

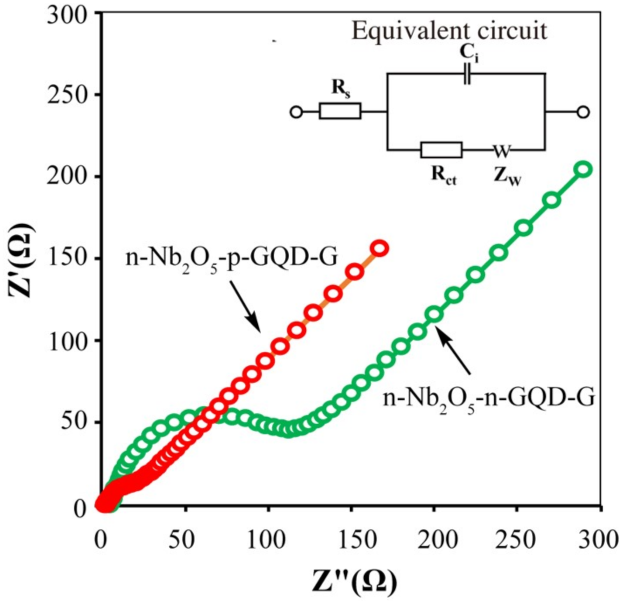

Fig. s13 EIS curves of n-Nb_2O_5-p-GQD-G and n-Nb_2O_5-n-GQD-G in 1M H_2SO_4 solution

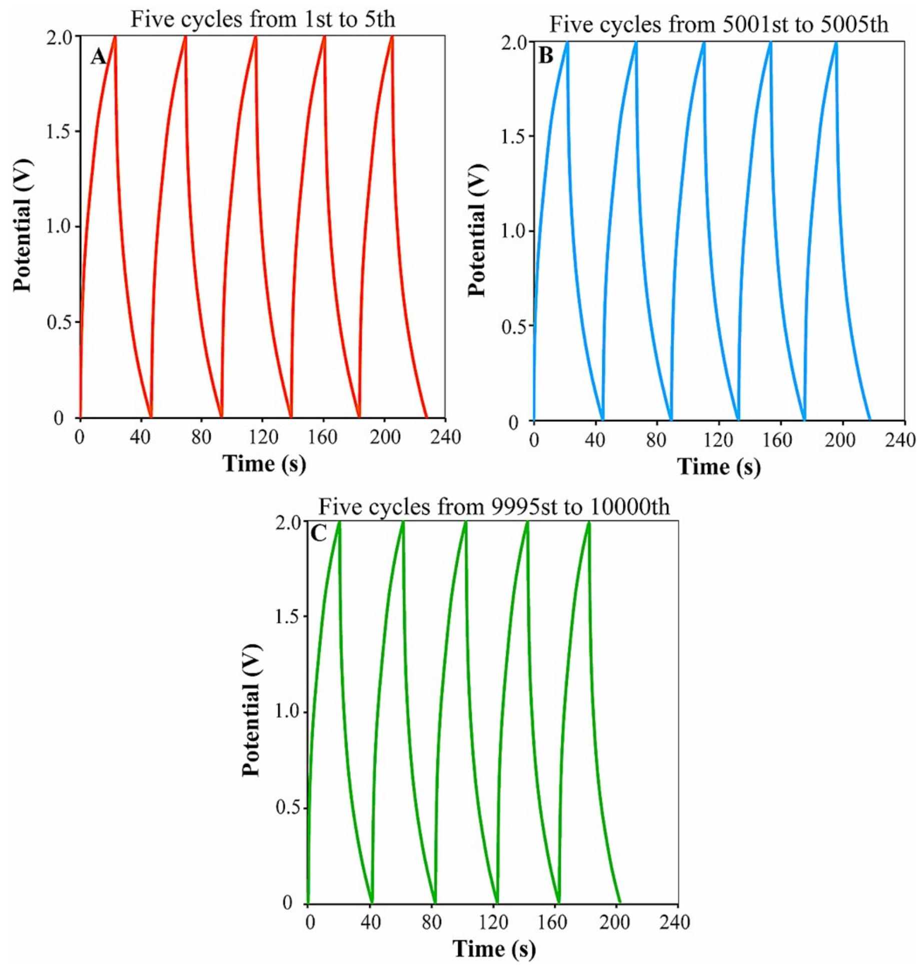

Fig. s14 The charge-discharge cures for the five cycles from 1st to 5th, the five cycles from 5001th to 5005th, and the five cycles from 9995th to 10000th

References

[1] N.N. Li, R.Y. Li, Q.S. Wang, Y.Q. Yang, X.L. Sun, G.L. Wang, Z.J. Li, Colorimetric detection of chlorpyrifos in peach based on cobalt-graphene nanohybrid with excellent oxidase-like activity and reusability, *J. Hazard. Mater.*, **2021**, 415, 125752.

[2] R.Y. Li, K.Y. He, Y.Q. Yang, H.Y. Zhu, **Z.J. Li**, Atomically dispersed RuO_2-tryptophan functionalized graphene quantum dot-graphene hybrid with double Schottky heterojunctions for high performance flexible supercapacitors, *Chem. Eng. J.*, **2021**, 426, 130893.

[3] X. Wang, C.Y. Yan, J. Yan, A. Sumboja, P.S. Lee, Orthorhombic niobium oxide nanowires for next generation hybrid supercapacitor device, *Nano Energy*, **2015**, 11, 765-772.

[4] Y. Dai, L.P. Ma, J.Q. Hu, J.H. Wang, H. Yan, H.Y. Zhang, H.Q. Wang, C.Y. Lai, W.R. Li, J.C. Zheng, Highly porous niobium oxide/carbon matrix materials with distinct pseudocapacitive performances in aqueous electrolytes, *Electrochim. Acta*, **2021**, 371, 137792.